

Novel free-form optical pairs for tunable focalizers

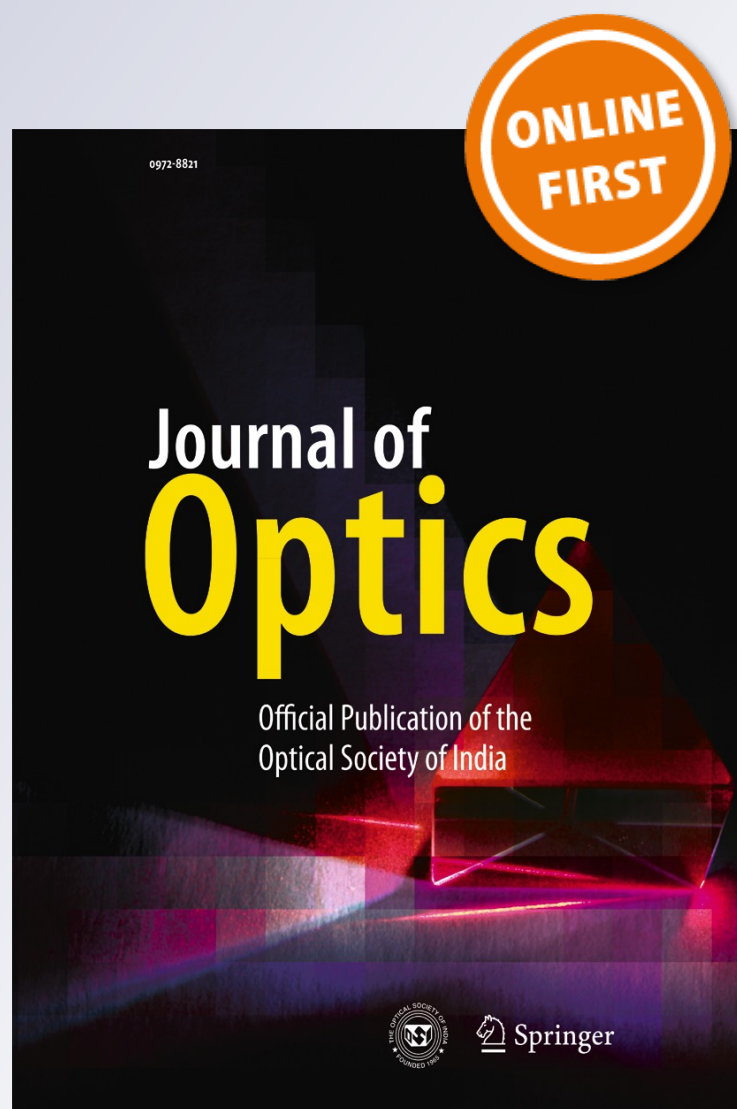
**Jorge Ojeda-Castañeda, Cristina
M. Gómez-Sarabia & Sergio Ledesma**

Journal of Optics

ISSN 0972-8821

J Opt

DOI 10.1007/s12596-014-0194-9



 Springer

Your article is protected by copyright and all rights are held exclusively by The Optical Society of India. This e-offprint is for personal use only and shall not be self-archived in electronic repositories. If you wish to self-archive your article, please use the accepted manuscript version for posting on your own website. You may further deposit the accepted manuscript version in any repository, provided it is only made publicly available 12 months after official publication or later and provided acknowledgement is given to the original source of publication and a link is inserted to the published article on Springer's website. The link must be accompanied by the following text: "The final publication is available at link.springer.com".

Novel free-form optical pairs for tunable focalizers

Jorge Ojeda-Castañeda · Cristina M. Gómez-Sarabia · Sergio Ledesma

Received: 14 March 2014 / Accepted: 31 March 2014
© The Optical Society of India 2014

Abstract We unveil the use of a pair of free-form refractive elements for optically implementing tunable phase delays, over several annularly distributed regions, which are here represented by a binary function. We show that there is a closely related technique, which is useful for controlling amplitude attenuations over selected annularly distributed regions. We combine our two proposals for describing a tunable radial Schlieren technique, as well as a controllable phase contrast technique.

Keywords Free-form optical elements · Tunable phase delays · Tunable Apodizers · Radial schlieren technique · Phase contrast method

Introduction

By moving axially some of the optical elements forming a varifocal system, one can modify the overall optical power. Zoom systems preserve the positions of one conjugate pair, while one changes the optical power [1]. And 2-conjugate zoom systems are able to preserve the positions of two independent conjugate pairs, while one changes the optical power [2].

Apparently Kitajima invented a different type of varifocal lenses [3, 4], by using two free-form elements working as a pair. This optical technique was later rediscovered, independently and almost simultaneously, by Alvarez [5] and Lohmann [6–8].

J. Ojeda-Castañeda (✉) · S. Ledesma
Engineering Division, Electronics Department, University of Guanajuato, Campus Salamanca, Campus Salamanca, Guanajuato, Mexico
e-mail: jojedacas@ugto.mx

C. M. Gómez-Sarabia
Digital Arts Department, University of Guanajuato, Campus Salamanca, Guanajuato, Mexico

Recently, we have revisited the Alvarez-Lohmann proposal for implementing several novel focalizers and some nonconventional apodizers by using optical elements that have helical modulations, or if you will vortex like amplitude variations [9, 10].

Here our aim is threefold. First, we unveil the use of a pair of free-form refractive elements for optically implementing tunable phase delays, over several annularly regions, which are here represented by a binary function. Second, we discuss a closely related technique for generating controllable amplitude variations, over pre-specified annularly regions. Third, we combine our two previous results for describing a tunable version of a radial Schlieren technique [11–14], and a tunable version of the phase contrast technique [15].

To our end, in Section 2, we describe the use of two masks that have helical phase delays over pre-specified annular regions. In Section 3, we extend the previous results to the generation of tunable absorption rings. In Section 4, we show that these results are useful for implementing a tunable, radial Schlieren technique; as well as a controllable phase contrast technique.

In Figs. 1 and 2, we display the schematics of an optical processor. At its Fraunhofer plane, we locate two independent spatial filters. One filter is a phase-only filter that is depicted in green color. Since we want to implement controllable phase delays, this phase-only filter has two refractive components that work as a pair.

Also at the Fraunhofer plane, of the optical processor, there is a second filter that is shown using gray levels. This is a tunable absorption device, which has two absorption masks working as a pair. In Section 2 we discuss the main features of the tunable phase-only filter; while in Section 3 we discuss the characteristics of the tunable absorption spatial filter.

Tunable phase delays over annular regions

In what follows, we describe the use of two free-form refractive elements, which work as a pair. If one introduces an in-

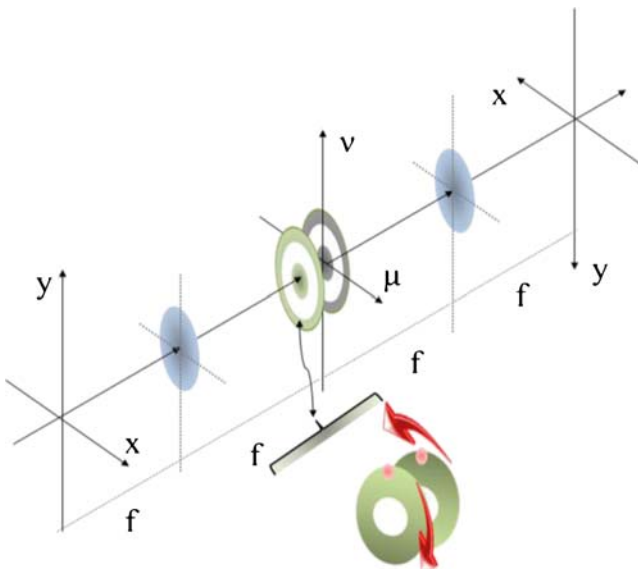


Fig. 1 Optical processor with a phase-only filter

plane rotation, between the elements of the pair, one can control the phase delay inside pre-specified annular regions. To our end, we assume that the complex amplitude transmittance of the first refractive element is

$$T_1(\rho, \varphi) = \exp\{ia\varphi B(\rho)\} \text{circ}\left(\frac{\rho}{\Omega}\right). \quad (1)$$

In Eq. (1) we include a constant phase factor that sets the maximum phase delay at the value $2\pi a$. The Greek letters ρ and φ denote, respectively, the radial spatial frequency and the polar angle on the pupil aperture. The maximum value of ρ is Ω , which denotes the cut-off spatial frequency of the

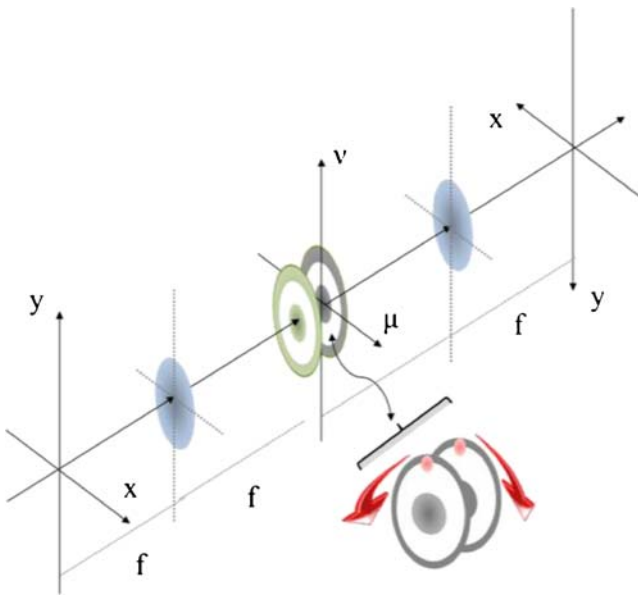


Fig. 2 Absorption pair located at the Fraunhofer plane of an optical processor

pupil aperture. Hence, the circular pupil aperture is represented by the circle function $\text{circ}(\rho/\Omega)$. Inside the pupil aperture we consider that there are some annular regions. We use a binary function $B(\rho)$ for locating these annular regions. Inside the regions of interest $B(\rho)=1$. Outside these regions, the function $B(\rho)=0$.

In Fig. 3 we show, with green color, the location of some annular regions, where the binary function, $B(\rho)$, is equal to unity.

Now, the complex amplitude transmittance of the second refractive element is

$$T_2(\rho, \varphi) = \exp\{-ia\varphi B(\rho)\} \text{circ}\left(\frac{\rho}{\Omega}\right). \quad (2)$$

After we have introduced an in-plane rotation (say by an angle β) between the elements of the pair, the overall complex amplitude transmittance is

$$\begin{aligned} P_{\text{phase}}(\rho, \varphi; \beta) &= T_1\left(\rho, \varphi + \frac{\beta}{2}\right) T_2\left(\rho, \varphi - \frac{\beta}{2}\right) \\ &= \exp\{ia\beta B(\rho)\} \text{circ}\left(\frac{\rho}{\Omega}\right). \end{aligned} \quad (3)$$

It is apparent from Eq. (3) that the overall complex amplitude transmittance is independent of the polar angle φ . Furthermore, we note that by selecting the value of the angle β , one can control the phase delay inside the regions where $B(\rho)=1$.

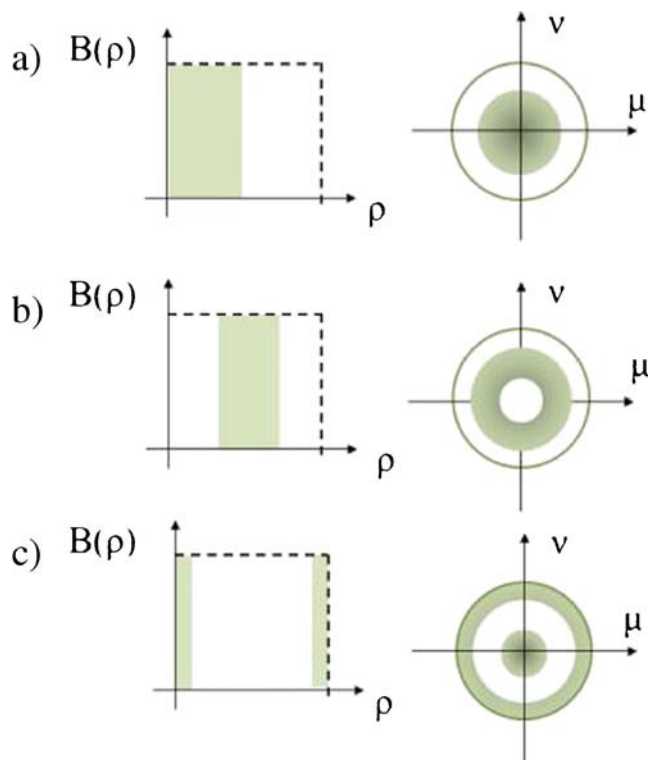
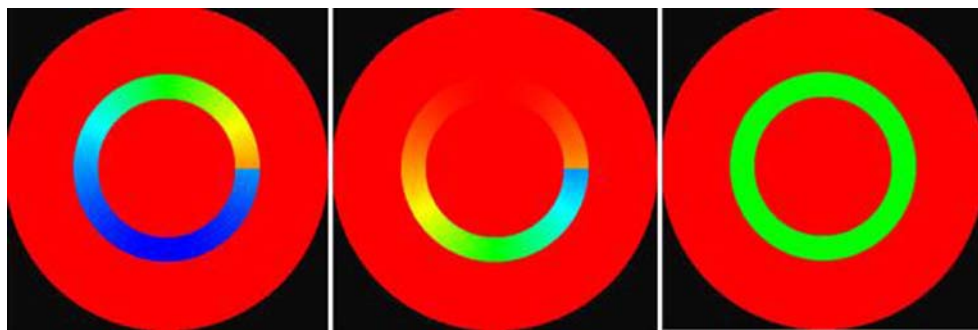


Fig. 3 Schematics for illustrating the use of the binary function $B(\rho)$

Fig. 4 Phase pairs and synthesized tunable phase delay



In Fig. 4, from left hand side to right hand side, we show pictures that display as color variations, the phase changes in each of the composing masks, as well as the resultant phase delay over a central ring. For this example, $a=1$, $\beta=\pi$. The center of the ring is at $\Omega / 2$; and the width of the ring is $\Omega / 10$.

Tunable absorption values over annular regions

Next we use two absorption masks, also working as a pair, for setting tunable absorption values inside pre-specified annular regions. Now, each amplitude mask has a helical amplitude variation, inside the regions where $B(\rho)=1$. The amplitude transmittance of the first absorption mask is

$$T_3(\rho, \varphi) = \exp\left\{-c\left(\frac{\varphi}{2\pi}\right)B(\rho)\right\} \text{circ}\left(\frac{\rho}{\Omega}\right). \tag{4}$$

In Eq. (4) we use the Latin letter c for representing a real number that specifies the maximum value of the attenuation coefficient, over the annular regions where the binary function $B(\rho)=1$. Since the amplitude transmittance varies linearly with the polar angle φ , and then the absorption mask has helical amplitude variations. The complex amplitude transmittance of the second absorption masks is

$$T_4(\rho, \varphi) = \exp(-c)\exp\left\{c\left(\frac{\varphi}{2\pi}\right)B(\rho)\right\} \text{circ}\left(\frac{\rho}{\Omega}\right). \tag{5}$$

We note the following. If the binary function $B(\rho)=1$, then the maximum amplitude transmittance is equal

to unity for $\varphi=2\pi$. If the binary function $B(\rho)=0$, the second mask has a uniform amplitude transmittance. If we use together the two above absorption masks after introducing an in-plane rotation, say by an angle γ , the overall amplitude transmittance is

$$P_{\text{attenuation}}(\rho, \varphi; \gamma) = T_3\left(\rho, \varphi + \frac{\gamma}{2}\right) T_4\left(\rho, \varphi - \frac{\gamma}{2}\right) = \exp\left\{-c\left[1 + \left(\frac{\gamma}{2\pi}\right)B(\rho)\right]\right\} \text{circ}\left(\frac{\rho}{\Omega}\right). \tag{6}$$

It is apparent from Eq. (6) that the overall complex amplitude transmittance is independent of the polar angle φ . Furthermore, by changing the value of γ , one can reduce the amplitude transmittance inside the regions where $B(\rho)=1$. In Fig. 5, along columns one and two respectively, we show the amplitude transmittances in Eqs. (4), (5) and (6).

Along the first line of Fig. 5, the two absorption masks (Column one and column two) are aligned, $\gamma=0$, then the two masks generate a uniform amplitude distribution; as shown along the first line third column. For this example, the center of the ring is at $\Omega/2$; the width of the ring is $\Omega/10$; and the attenuation coefficient is $c=1.1$. The amplitude variations in Fig. 5 are displayed as pseudo-colors in Fig. 6.

Next, we combine the previous results for setting two tunable phase imaging techniques.

Fig. 5 Amplitude variations as gray level pictures

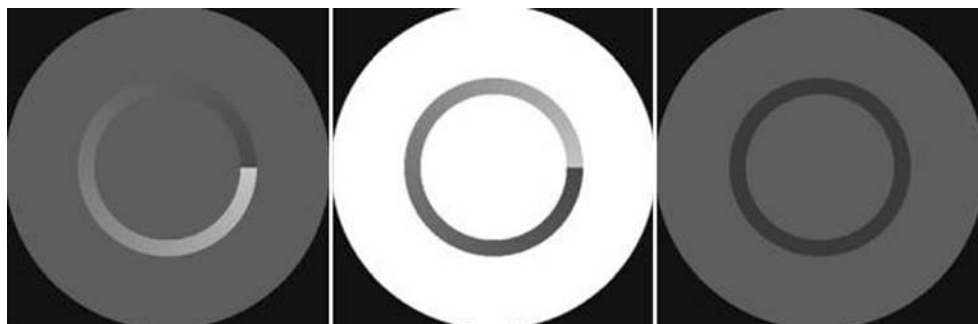
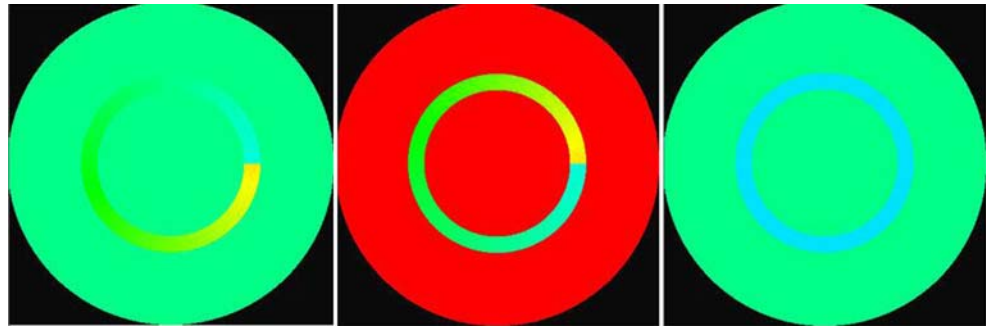


Fig. 6 Pseudo-color display of the proposed amplitude masks



Phase rendering techniques

In what follows, for the sake of clarity, we discuss initially the 1-D case in Cartesian coordinates. Then, we employ a linear geometrical transformation for obtaining the 2-D case with radial symmetry.

For rendering visible a thin phase structure, it is convenient to recognize the following. There is an effective transfer function that describes the process of mapping weak phase variations into irradiance variations [16–20]. For coherent illumination, the effective transfer function is

$$H(\xi) = \frac{1}{|Q(0)|^2} \{Q^*(0)Q(\xi) - Q(0)Q^*(\xi)\}. \tag{7}$$

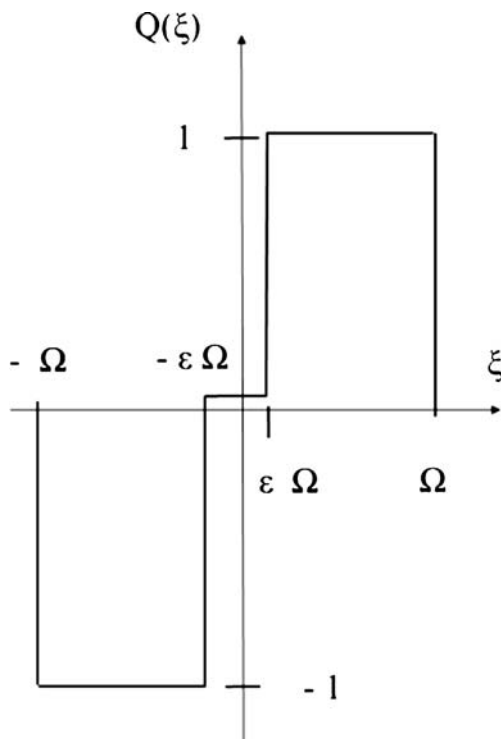


Fig. 7 Complex amplitude transmittance of the 1-D Schlieren mask under discussion

In Eq. (7) we use the Greek letter ξ for denoting the spatial frequency along the 1-D, pupil aperture. The function $Q(\xi)$ describes the 1-D generalized pupil function representing the spatial filter. If $|\xi| > \Omega$, then $Q(\xi) = 0$. As indicated in references [19, 20], for implementing a useful Schlieren technique, one needs the following the generalized pupil function

$$\begin{aligned} Q(\xi) &= -1, & \text{if } -\Omega \leq \xi \leq -\epsilon \Omega \\ Q(\xi) &= e^{-c}, & \text{if } -\epsilon \Omega \leq \xi \leq \epsilon \Omega \\ Q(\xi) &= 1, & \text{if } \epsilon \Omega \leq \xi \leq \Omega. \end{aligned} \tag{8}$$

In Fig. 7 we depict the complex amplitude transmittance in Eq. (8). The Greek letter ϵ denotes a real number; such that $0 < \epsilon \ll 1$; which is useful for setting the interval $|\xi| < \epsilon \Omega$. Here it is relevant to remember that by using attenuation at the center of the Fraunhofer diffraction pattern, one can enhance weak irradiance variations.

Now, by substituting Eq. (8) in Eq. (7) we obtain that the effective transfer function becomes

$$\begin{aligned} H(\xi) &= -2e^c & \text{if } -\Omega \leq \xi \leq -\epsilon \Omega \\ H(\xi) &= 0 & \text{if } -\epsilon \Omega \leq \xi \leq \epsilon \Omega \\ H(\xi) &= 2e^c & \text{if } \epsilon \Omega \leq \xi \leq \Omega. \end{aligned} \tag{9}$$

It is apparent from Eq. (9) that the Schlieren mask implements a bandlimited Hilbert transformation, which has a

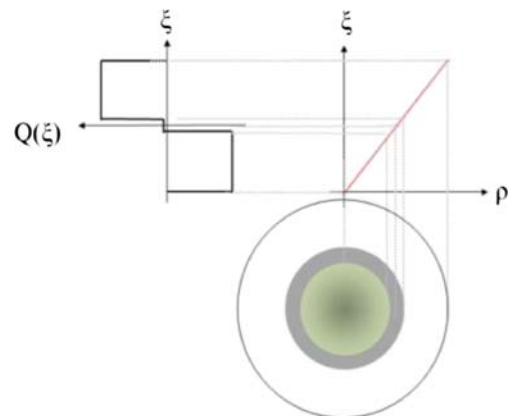
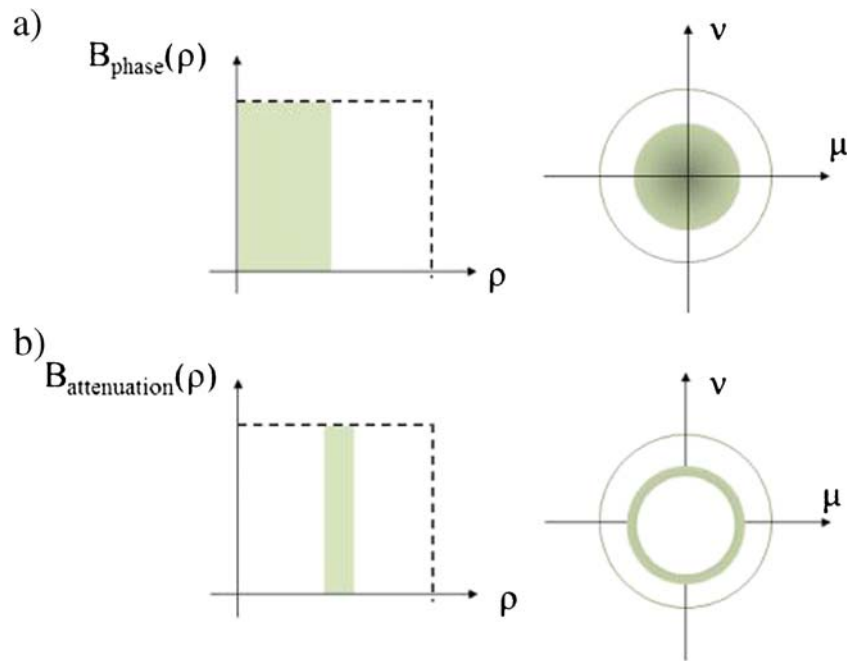


Fig. 8 Linear geometrical mapping for obtaining the radially symmetric Schlieren mask

Fig. 9 Location of the binary regions for the: **a** phase-only filter, **b** attenuation filter



relative enhancement factor $2 \exp(c)$. This enhancement factor is caused by the use of the absorption strip at the center of the Fourier spectrum.

Now, we perform a linear geometrical transformation for obtaining the radially symmetric, 2-D complex amplitude transmittance. In mathematical terms, as is depicted in Fig. 8, we define the geometrical transformation

$$\rho = 0.5(\xi + \Omega); \quad P(\rho) = Q(\xi). \quad (10)$$

It is apparent from Eq. (10), and indeed from Fig. 8, that the 2-D, radially symmetric, generalized pupil function is

$$P(\rho) = - \text{circ}\left(\frac{2\rho}{(1-\varepsilon)\Omega}\right) + e^{-c} \left\{ \text{circ}\left(\frac{2\rho}{(1+\varepsilon)\Omega}\right) - \text{circ}\left(\frac{2\rho}{(1-\varepsilon)\Omega}\right) \right\} + \left\{ \text{circ}\left(\frac{\rho}{\Omega}\right) - \text{circ}\left(\frac{2\rho}{(1+\varepsilon)\Omega}\right) \right\}. \quad (11)$$

From Eq. (11) it is straightforward to identify the binary functions that are needed for setting first the tunable phase delay, and second the tunable attenuation masks.

As is depicted in Fig. 9a, for the phase delay, we set

$$B_{\text{phase}}(\rho) = \text{circ}\left(\frac{2\rho}{(1-\varepsilon)\Omega}\right). \quad (12)$$

Hence, the free-form refractive elements have the following complex amplitude transmittances

$$T_1(\rho, \phi) = \exp\left\{ ia\phi \text{circ}\left(\frac{2\rho}{(1-\varepsilon)\Omega}\right) \right\} \text{circ}\left(\frac{\rho}{\Omega}\right), \quad (13)$$

$$T_2(\rho, \phi) = \exp\left\{ ia\phi \text{circ}\left(\frac{2\rho}{(1-\varepsilon)\Omega}\right) \right\} \text{circ}\left(\frac{\rho}{\Omega}\right). \quad (14)$$

Thus, the overall complex amplitude transmittance is

$$P_{\text{phase}}(\rho; \beta) = \exp\left\{ ia\beta \text{circ}\left(\frac{2\rho}{(1-\varepsilon)\Omega}\right) \right\} \text{circ}\left(\frac{\rho}{\Omega}\right). \quad (15)$$

It is now apparent that by changing the angle β from zero to π/a , we can introduce a phase delay of π , over the inner circle on the pupil.

In a similar fashion, see Fig. 9b, one can find that for implementing the necessary attenuation factor (over the middle ring) the binary function is

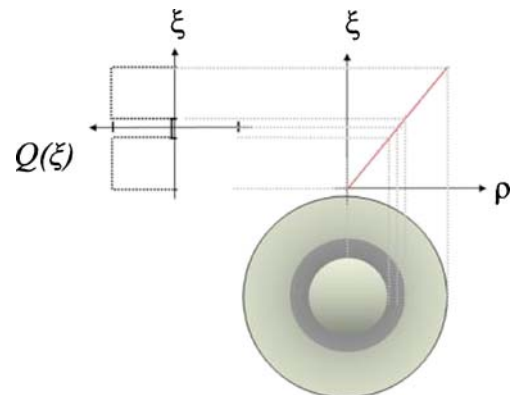
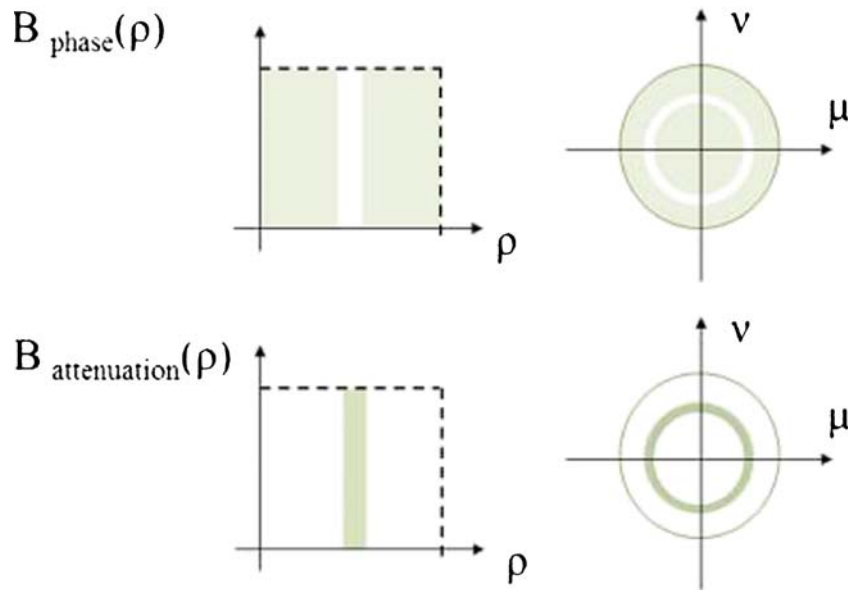


Fig. 10 Linear geometrical mapping for obtaining for the radially symmetric phase contrast method

Fig. 11 Location of the binary regions: **a** phase-only filter, **b** attenuation filter



$$B_{attenuation}(\rho) = circ\left(\frac{2\rho}{(1+\varepsilon)\Omega}\right) - circ\left(\frac{2\rho}{(1-\varepsilon)\Omega}\right). \quad (16)$$

Then, for the absorption pair, the overall complex amplitude transmittance is

$$P_{attenuation}(\rho, \phi; \gamma) = \exp(-c) \exp\left\{-c\left(\frac{\gamma}{2\pi}\right)\left[circ\left(\frac{2\rho}{(1+\varepsilon)\Omega}\right) - circ\left(\frac{2\rho}{(1-\varepsilon)\Omega}\right)\right]\right\}. \quad (17)$$

Hence, by changing the angle γ we can increase the attenuation factor over the middle ring.

Finally, we notice that our proposal can also be applied to implement the renowned phase contrast method. For this later example the diagram for the geometrical transformation, which was depicted before in Fig. 8, is the one in Fig. 10.

The binary function for both the tunable phase delay and the tunable attenuation masks are depicted in Fig. 11a, b respectively.

For the phase delay, the binary function is

$$B_{phase}(\rho) = circ\left(\frac{\rho}{\Omega}\right) - \left\{circ\left(\frac{2\rho}{(1+\varepsilon)\Omega}\right) - circ\left(\frac{2\rho}{(1-\varepsilon)\Omega}\right)\right\}. \quad (18)$$

Next, we use the result in Eq. (18) for specifying the pair of free-form refractive elements. For the first refractive element, the complex amplitude transmittance is

$$T_1(\rho, \phi) = \exp\{ia\phi B_{phase}(\rho)\} circ\left(\frac{\rho}{\Omega}\right). \quad (19)$$

And for the second refractive element, the complex amplitude transmittance is

$$T_2(\rho, \phi) = \exp\{-ia\phi B_{phase}(\rho)\} circ\left(\frac{\rho}{\Omega}\right). \quad (20)$$

The overall complex amplitude transmittance is

$$P_{phase}(\rho; \beta) = \exp\{ia\beta B_{phase}(\rho)\} circ\left(\frac{\rho}{\Omega}\right). \quad (21)$$

Therefore, by changing the angle β from zero to $\pi/2$, we can introduce the desired phase delay of $\pi/2$, over the first circle and over the exterior ring, on the pupil aperture; as is done in a similar fashion in references [21, 22].

Once again, for implementing the necessary attenuation factor over the middle ring, the binary function is

$$B_{attenuation}(\rho) = circ\left(\frac{2\rho}{(1+\varepsilon)\Omega}\right) - circ\left(\frac{2\rho}{(1-\varepsilon)\Omega}\right). \quad (22)$$

And consequently, for the attenuation pair, the overall complex amplitude transmittance reads as the mathematical expression in Eq. (17). By changing the angle γ , one can introduce the desired attenuation on the middle ring on the pupil aperture.

Conclusions

We have discussed an optical method for setting spatial filters, which have controllable complex amplitude transmittances over selected annular regions. To this end, we have described the use of optical elements that have helical complex amplitude transmittances. Or equivalently, the proposed filters have vortex like complex amplitude variations.

We have indicated that one can implement a tunable phase-only filter, by using two free-form refractive elements. By introducing an in-plane rotation between the free-form refractive pair, one can control the phase delay over the selected annular regions.

On the other hand, we have indicated that there is a closely related technique that is useful for implementing absorption values over selected annular regions. We have indicated that these annular regions can be usefully specified by another binary function. At the selected annular regions, the masks have helical amplitude variations. That is, the amplitude transmittance varies linearly with the polar angle.

For illustrating the capabilities of our proposal, we have discussed the combination of tunable phase masks with controllable absorption masks for implementing two, radially symmetric phase rendering techniques.

We gratefully acknowledge the financial support of CoNaCyT (grant 157673), as well as the support from the University of Guanajuato (UGto-CIO agreement).

References

1. R. Kingslake, R.B. Johnson, *Lens Design Fundamentals* (Academic, Amsterdam, 2010)
2. H.H. Hopkins, 2-Conjugate Zoom Systems, in *Optical Instruments and Techniques*, ed. by J. Home Dickson (Oriel Press, Newcastle, 1970)
3. I. Kitajima, Improvement in lenses. British Patent 250, 268 (July 29, 1926)
4. W.T. Plummer, J.G. Baker, J. van Tassell, Photographic optical systems with nonrotational aspheric surfaces. *Appl. Opt.* **38**, 3572–3592 (1999)
5. L.W. Alvarez, Two-element variable-power spherical lens. US Patent 3,305, 294 (December 3, 1964)
6. Adolf W. Lohmann, Lente a focale variabili. Italian Patent 727,848 (June 19, 1964)
7. A. W. Lohmann, Improvements relating to lenses and to variable optical lens systems formed for such a lens. Patent Specification 998, 191, London (1965)
8. A.W. Lohmann, A new class of varifocal lenses. *Appl. Opt.* **9**, 1669–1671 (1970)
9. J. Ojeda-Castaneda, S. Ledesma, C.M. Gómez-Sarabia, Tunable Apodizers and Tunable Focalizers using helical pairs. *Photonics Lett. Pol.* **5**, 20–22 (2013)
10. J. Ojeda-Castaneda, C.M. Gómez-Sarabia, *Tunable Focalizers: Axicons, Lenses and Axilenses*. eds. J. Ojeda-Castaneda, M.J. Yzuel, R.B. Johnson. Proceedings SPIE 8833, 8833061–8833066 (2013)
11. J.K.T. Eu, A.W. Lohmann, Isotropic Hilbert spatial filtering. *Opt. Commun.* **9**, 257 (1973)
12. J. Ojeda-Castaneda, L.R. Berriel-Valdos, Classification scheme and properties of the Schlieren techniques. *Appl. Opt.* **18**, 3338–3341 (1979)
13. J. Ojeda-Castañeda, Foucault, wire and phase-modulation tests, Chapter 8, in *Optical Shop Testing*, ed. Daniel Malacara (Wiley, Hoboken, 2007), pp. 291–292
14. J. Ojeda-Castaneda, E. Jara, Isotropic Hilbert transform by anisotropic spatial filtering. *Appl. Opt.* **25**, 4035–4038 (1986)
15. F. Zernike, Phase contrast, a new method for the microscopic observation of transparent objects. *Physica* **9**, 686 (1942). reprinted in *Achievements in Optics*, ed. A. Bouwers (Elsevier, Amsterdam, 1950), pp. 116–135
16. E. Menzel, Die Abbildung von Phasenobjekten in der Optischen Übertragungstheorie, in *Optics in Metrology*, ed. by P. Mollet (Pergamon Press, Oxford, 1960), pp. 283–293
17. E. Menzel, W. Mirandé, I. Weingaertner, *Fourier-Optik und Holographie* (Springer, Wien, 1973), pp. 77–79
18. J. Ojeda-Castaneda, Spatial Filtering Properties of the Methods Employed to Detect Phase Structures, Under Partially Coherent Illumination, in *Optica Hoy y Mañana*, ed. by J. Bescos, A. Hidalgo, L. Plaza, J. Santamaria (Sociedad Española de Optica, ICO, Madrid, 1978), pp. 287–290
19. J. Ojeda-Castaneda, A proposal to classify methods employed to detect thin phase structures, under coherent illumination. *Opt. Acta* **27**, 917–929 (1980)
20. J. Ojeda-Castaneda, Necessary and sufficient conditions for thin phase imagery. *Opt. Acta* **27**, 905–915 (1980)
21. S. Bernet, A. Jesacher, S. Fuerhapter, C. Maurer, M. Ritsch-Marte, Quantitative imaging of complex samples by spiral phase contrast microscopy. *Opt. Express* **14**(9), 3792–3805 (2006)
22. S. Bernet, M. Ritsch-Marte, Optical device with a pair of diffractive optical elements. US Patent 0134869 A1 (2010)